Thermal and Exergy Analysis in UPS and Battery Rooms by Numerical Simulations

Carol Caceres[*], Alfonso Ortega[**], Luis Silva-Llanca[+], Gerard F. Jones[***], Nicholas Sapia[++]
Villanova University
Villanova, PA, USA, 19085
Email: [*]acacere4@villanova.edu
[**]alortega@scu.edu
[+]lsilva@usarena.cl
[***]gerard.jones@villanova.edu
[++]nicholas.sapia@verizonwireless.com

ABSTRACT

UPS (Uninterruptible Power Supply) units and batteries are essential subsystems in data centers or telecom industries to protect equipment from electrical power spikes, surges and power outages. UPS units handle electrical power and dissipate a large amount of heat, and possess a high efficiency. Therefore, cooling units (e.g., CRACs) are needed to manage the thermal reliability of this equipment. On the other hand, battery operating conditions and reliability are closely related to the ambient temperature according to battery manufacturers; reliability increases when the ambient room temperature is around 25ºC. This study analyzed different room configurations and scenarios using the commercial CFD software 6Sigma Room DCX™. As a first approach, we evaluated the thermal behavior and cooling degradation using standard thermal performance metrics SHI (Supply Heat Index) and RHI (Return Heat Index). These are frequently implemented in data centers to measure the level of mixing between cold and hot air streams. The results from this evaluation showed that standard cooling practices are inefficient, as values for the two metrics differed considerably from industry recommendations. We also considered a metric from the second law of thermodynamics using exergy destruction. This technique allowed us to find the mechanisms that increase entropy generation the most, including viscous shear and air stream mixing. Reducing exergy destruction will result in lessening lost thermodynamic work and thus reduce energy required for cooling. Typically, UPS and batteries are located in different rooms due to the hydrogen generation by the batteries. The integration of both equipment in the same room is a new concept, and this study aims to analyze the thermal performance of the room. Adding controllability showed improvements by reducing the exergy destruction due to viscous dissipation while slightly increasing thermal mixing in the rooms. Ducting the return flows to avoid flow mixing increased pressure drop, but reduced heat transfer between the hot and cold air streams, which in turn, improved the thermal performance. In the study, we determined the optimal configuration and possible strategies to improve cooling while maintaining desirable battery temperatures.

KEY WORDS: Data Center, UPS, Lead Acid Battery, Thermodynamics, Exergy Destruction, CFD

NOMENCLATURE

c_p	Specific heat, J/kg-K
k	Thermal conductivity, W/m-K
$\dot{m}$	Mass flow rate, kg/m^3
P	Pressure, Pa
$\dot{S}'''_{Gen}$	Entropy production, W/m^3
T	Temperature, ºC
$\dot{W}$	Shaft power, W
$\dot{Q}$	Heat transfer rate, W

Greek symbols

α	Thermal diffusivity, m^2/s
α_t	Turbulent thermal diffusivity, m^2/s
ε	Turbulence dissipation rate
ρ	Air density, kg/m^3
κ	Turbulence kinetic energy, J/kg
$\dot{\psi}'''$	Exergy rate per volume, W/m^3
$\dot{\psi}$	Exergy rate, W

Subscripts

in	inlet
out	outlet
o	Dead state
Gen	Generation
Dest	Destruction

Superscripts

CRAC	Computer room air conditioner
UPS	Uninterruptible power supply

INTRODUCTION

Generally, most attention in a data center goes to the server room. Known thermal practices are generally applied to the rooms where IT is located as well as thermal performance metrics. An extensive review of thermal metrics for IT equipment rooms was made by Capozzoli et al. [1] to understand the basics and provide a critical review. Studies about UPS and batteries from a thermal point of view are not found in the literature. The integration of equipment such as UPS and batteries in the same room that is analyzed in this paper is therefore not a common practice.

The UPS and battery are crucial components in data center facilities. UPS units convert electrical power from AC to DC current, while batteries store electrical energy as backup. Also, these two technologies are commonly found in different locations in data centers which use lead acid-based batteries. Vented lead-acid and valve-regulated lead acid batteries are

the typical types of batteries used in data centers. Most of the standards and practices used in battery rooms are about safety and operability. For example, NFPA 70 [2] explains safety conditions for battery plants regarding fire emergencies. On the other hand, the IEEE 2002a [3] mainly regards ventilation methods. Ambient temperature is the thermal parameter for batteries. According to ASHRAE [4], batteries working at normal conditions, or float voltages, dissipate heat to the ambient, which is generally negligible. Even during the charging and discharging processes, the heat released to the surrounding area is neglected. Furthermore, battery room temperature must be controlled, for North America, ASHRAE [4] recommends 77ºF (25ºC) to achieve maximum battery reliability and maximum discharging capacity. IEEE 2005 [5] mentions that when batteries work at low temperatures at around 25ºC, the discharge capacities and life expectancy are reduced, while the opposite occurs at higher temperatures.

Uninterruptible power supply units and electrical distribution systems have high efficiencies, but the losses by heat are considerable because these units manage high electrical power. According to APC [6], 19% of heat rejection to the rooms is attributed to UPS and power distribution systems. Because UPS units handle large powers, they can operate at higher temperatures than the batteries. However, in this paper the batteries and UPS are installed in the same room, so cooling is required.

Due to the lack of information to evaluate the cooling performance in the rooms having both UPS and batteries, two different approaches were considered. For thermal evaluation, the SHI and RHI metrics developed by Sharma et al. [7] were used. These values measure the level of cooling degradation in the room associated with the hot and cold air stream mixing. This approach evaluates the enthalpy increase from cooling and the enthalpy decrease from heat rejection in the room at the maximum possible temperature. Mixing problems can be detected with these metrics. However, since SHI and RHI are lumped quantities and not local, the causes of the mixing and the locations of the zones of mixing are not detected with them.

Efficiency can be maximized using the second law of thermodynamics to calculate the entropy generated and quantify the available work, also called exergy. The concepts of exergy and exergy destruction have been applied to data centers by different authors, all of whom maintain a focus on server rooms. Shah et al.[8], made an exergy study on a data center in order to identify the irreversibilities. Inefficiencies were found and attributed to flow work, recirculation, and short circuiting. The maximum exergy destruction was measured at the CRAC. Shah et al.[9-15] did more studies using CFD simulations to estimate exergy losses and obtain an optimal flow rate that the CRAC must supply. On the other hand, figure of merits were developed based on the exergy concept, but these parameters were applied at the chip level.

CFD software, based on the first law of thermodynamics and the equations of motion for air, is ideal for detailed exploration of the locations and sources of exergy destruction. An entropy transport equation was introduced into CFD analysis by Kock and Herwig [16, 17] and [18]. These authors introduced the entropy production analysis in turbulent flow, which is the common air-flow behavior in data centers. The method proposed by Kock and Herwig was used in this paper to evaluate the exergy destruction in battery and UPS rooms.

MOTIVATION

The integration of battery and UPS in the same room is a new concept. The motivation of this work is to evaluate the thermal performance of different room configurations. Hydrogen generation by the batteries is considered as possible future work.

METHODOLOGY

Equipment, Room Configuration and Scenarios Simulated

Today, numerical tools such as CFD are widely used to analyze problems when it is not possible or practical to do experiments or real measurements. The thermal evaluation of battery and UPS units was made through the commercial CFD software 6Sigma Room DCX™, developed by Future Facilities [19].

Three types of room configurations were designed and studied with CFD. Equipment present in the rooms is shown in Table 1.

Table 1. Equipment used in the Rooms.

Air Cooling Units	CRAC Liebert DA085
Power Distribution Units	PDU Liebert PPC 300
Uninterruptible Power Supply	UPS Liebert NXL 250
Batteries	Data Safe 2DCX-35

Layouts were modeled in 3D for three room configurations as discussed below. The equipment in Table 1 is available in the 6Sigma Room DCX library. Consistent with the literature for most of the cases simulated, the battery heat generation is considerable negligible. Batteries are considered as flow blockages that influence the flow pattern due to the geometry. Heat dissipation by the UPS units is considered 50% of the maximum heat dissipation, assuming that this equipment works between 40% and 80% of its capacity.

Scenarios were studied according to the number of CRACs installed in the room and which ones are operational (see Table 2). More than one CRAC in a room is required in case of a CRAC failure. An air flow control strategy was used. A proportional controller is assumed because it is an effective controller and the model for it is available in the software. It was configured based on a minimum-recommended air flow for the DA085 unit of 55% of maximum air flow rate.

a)

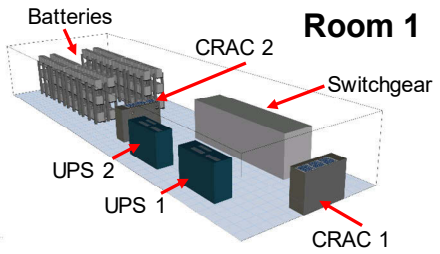

b)

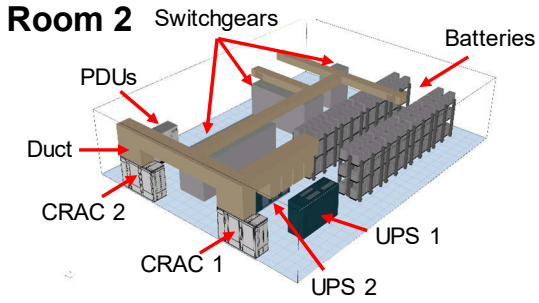

c)

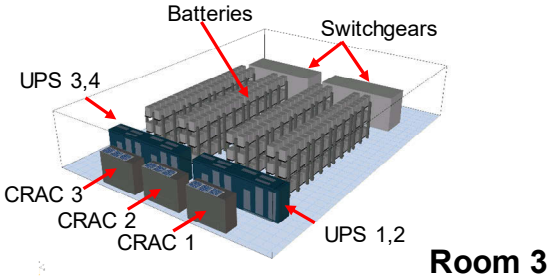

Figure 1. Room configuration. a) Room 1 has 2 CRAC and, 2 UPS units, b) Room 2 has 2 CRAC, 2 PDU and, 2 UPS and, c) Room 3 has 3 CRAC and 4 UPS.

Table 2. Scenarios simulated according to CRACs working.

		Operation		
	Scenarios	CRAC 1	CRAC 2	CRAC 3
Room 1	1	ON	ON	-
	2	OFF	ON	-
	3	ON	OFF	
Room 2	1	ON	ON	-
	2	OFF	ON	-
	3	ON	OFF	
Room 3	1	ON	ON	ON
	2	OFF	ON	ON
	3	ON	ON	OFF
	4	ON	OFF	ON

Based on safety considerations, we considered the supply of fresh air to the rooms as in the IEEE 484 standard [3]. Since the required air flow rate is just 15% of the air supplied by the CRAC units in most cases, the injection of outside air is neglectable in our calculations. Furthermore, the concentration of hydrogen molecules is avoided with a minimum air flow rate movement in the room due to hydrogen properties, IEEE standard [3].

Supply Heat Index and Return Heat Index

Most of the data center thermal performance metrics that exist today apply to server rooms. Popular metrics to measure thermal cooling performance are the Supply Heat Index (SHI) and Return Heat Index (RHI), Sharma et al. [7]. Applying these metrics to the rooms studied here, the ideal temperature at the UPS inlet is equal to the outlet CRAC temperature. Also, the outlet temperature from the UPS must be equal to that entering the CRAC. On other words, the heat rejected by the CRAC is the same heat dissipated by the UPS units. For the ideal case, SHI is 0 and RHI is 1.

The metric expressions were adjusted to correspond to the equipment in the rooms that we modeled and are defined as

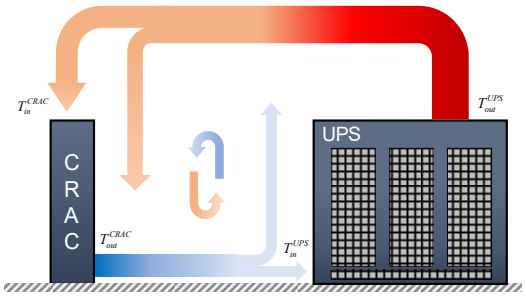

Figure 2. Temperatures for SHI and RHI metrics.

$$\mathrm{SHI} = \sum \frac{T_{in}^{UPS} - T_{out}^{CRAC}}{T_{out}^{UPS} - T_{out}^{CRAC}} \quad (1)$$

$$\mathrm{RHI} = \sum \frac{\dot{m}^{CRAC} \cdot c_p}{\dot{m}^{UPS} \cdot c_p} \frac{\left(T_{in}^{CRAC} - T_{out}^{CRAC}\right)}{\left(T_{out}^{UPS} - T_{out}^{CRAC}\right)} \quad (2)$$

$$\mathrm{SHI} + \mathrm{RHI} = 1 \quad (3)$$

Capozzoli et al. [1], note that SHI less than 0.2 and RHI greater than 0.8 correspond to good performance.

According to these expressions, the numerator for SHI is the enthalpy increase or decrease due to the air infiltrated at different temperatures differing from the ideal scenario. In the case of RHI, the enthalpy rise is observed in the denominator and the numerator is the total heat rejected. Both metrics can be used to evaluate thermal management, energy, and cooling efficiency. It is clear that the enthalpy increase due hot air infiltration in the cooling delivery to the UPS and the decreasing of heat rejection by the CRAC units is due to the existence of mixing and short circuiting that generate entropy. SHI and RHI are simple to implement either with CFD solutions or with real data once temperature readings are obtained.

Given that SHI and RHI produce lumped results (a single number for the entire room), it is not possible to identify the locations nor the sources of inefficiencies. We must resort to CFD results to obtain these.

Entropy Production in Turbulent Flows for CFD Models

The entropy production was calculated following the Kock and Herwig [16-18] method. The entropy transport equation is solved after solving the k-ε model for a turbulent flow. CFD methods solve the equations for mass, momentum, and energy conservation. The entropy equation is not solved. According to Kock and Herwig it is not necessary solve the entropy equation to obtain the entropy production. Four terms appear that produce entropy in turbulent flows when using the k-ε turbulence model

Table 3. Mechanisms that produce entropy, obtained from the k-ε turbulence model.

$\dot{S}'''_{Gen,\bar{D}}$	Entropy production rate by direct dissipation
$\dot{S}'''_{Gen,D'}$	Entropy production rate by indirect dissipation
$\dot{S}'''_{Gen,\bar{C}}$	Entropy production rate by heat conduction with mean temperature gradients
$\dot{S}'''_{Gen,C'}$	Entropy production rate by heat transfer with fluctuating temperature gradients

The Kock and Herwig model is

$$\dot{S}'''_{Gen,\bar{D}} = \frac{\mu}{\bar{T}}\left[\begin{array}{c} 2\left\{\left(\frac{\partial \bar{u}}{\partial x}\right)^2+\left(\frac{\partial \bar{v}}{\partial y}\right)^2+\left(\frac{\partial \bar{w}}{\partial z}\right)^2\right\}+ \\ \left(\frac{\partial \bar{u}}{\partial y}+\frac{\partial \bar{v}}{\partial x}\right)^2+\left(\frac{\partial \bar{u}}{\partial z}+\frac{\partial \bar{w}}{\partial x}\right)^2+\left(\frac{\partial \bar{v}}{\partial z}+\frac{\partial \bar{w}}{\partial y}\right)^2 \end{array}\right] \quad (4)$$

$$\dot{S}'''_{Gen,D'} = \frac{\rho\varepsilon}{\bar{T}} \quad (5)$$

$$\dot{S}'''_{Gen,\bar{C}} = \frac{k}{\bar{T}^2}\left[\left(\frac{\partial \bar{T}}{\partial x}\right)^2+\left(\frac{\partial \bar{T}}{\partial y}\right)^2+\left(\frac{\partial \bar{T}}{\partial z}\right)^2\right] \quad (6)$$

$$\dot{S}'''_{Gen,\bar{C}} = \frac{\alpha_t}{\alpha}\frac{k}{\bar{T}^2}\left[\left(\frac{\partial \bar{T}}{\partial x}\right)^2+\left(\frac{\partial \bar{T}}{\partial y}\right)^2+\left(\frac{\partial \bar{T}}{\partial z}\right)^2\right] \quad (7)$$

Expression (4) and (6) are obtained directly from the mean velocities and temperatures, are called direct because they are obtained from the mean flow field. On the other hand, (5) and (7) are derived from turbulence dissipation and are called indirect. The indirect terms come from the fluctuating character of a turbulent flow. The direct method is alternately described by Bejan [20] as differential analysis, describing in details the methodology. Silva-Llanca et al. [21,22] analyzed a data center using CFD and validated results from the Kock and Herwig model with experimental data.

Only the entropy generation for the air flow domain in the room is calculated using the above model. The final exergy destruction expression is obtained per unit of volume as

$$\dot{\psi}'''_{Dest,Visc} = T_o \cdot \left(\dot{S}'''_{Gen,\bar{D}} + \dot{S}'''_{Gen,D'}\right) \quad (8)$$

$$\dot{\psi}'''_{Dest,Heat} = T_o \cdot \left(\dot{S}'''_{Gen,\bar{C}} + \dot{S}'''_{Gen,C'}\right) \quad (9)$$

From Eqs. (8) and (9) we obtain the total exergy destruction in the room due to the direct and indirect dissipation, which are the terms that generates the entropy and the dead state temperature T_o. Therefore, the exergy destruction obtained with this method can be visualized as a contour, allowing us to detect zones where the exergy is destroyed by the mechanisms on which Eqs. (4), (5), (6) and (7) are based. The total exergy destruction rate in the room by the flow circulating in the room is

$$\dot{\psi}_{Dest,Total} = T_o\left\{\sum\left(\begin{array}{c}\dot{S}'''_{Gen,\bar{D}}+\dot{S}'''_{Gen,D'}+ \\ \dot{S}'''_{Gen,\bar{C}}+\dot{S}'''_{Gen,C'}\end{array}\right)\Delta x\Delta y\Delta z\right\} \quad (10)$$

Equation (10) calculates the total exergy destruction in the domain that the flow circulates by calculating the entropy production summation by cells.

Entropy Production by the CRAC units

Exergy destruction by the CRAC units is also considered. Average properties were used to obtain the exergy destruction for the inlet and outlet for air conditioning units. Figure 3 shows the control volume used to calculate the exergy destruction for this equipment.

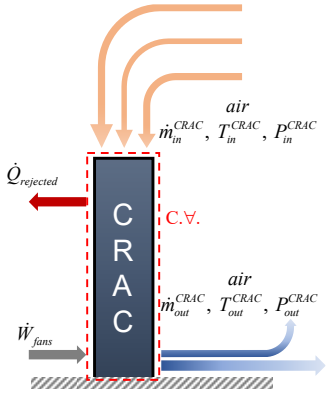

Figure 3. CRAC control volume. Exergy analysis.

From this figure, the equation to calculate the exergy destruction by the CRACs may be written from a combination of the First and Second laws of thermodynamics

$$\dot{\psi}_{Dest}^{CRAC} = T_o \cdot \dot{m}^{CRAC}\left(c_p \ln\left(\frac{T_{air}^{out}}{T_{air}^{in}}\right) - R\ln\left(\frac{P_{air}^{out}}{P_{air}^{in}}\right)\right) + \dot{W}_{fans} + \dot{m}^{CRAC} c_p\left(T_{air}^{in} - T_{air}^{out}\right) \quad (11)$$

Equation (11) represents the exergy destroyed just for the CRAC. It includes both heat transfer and irreversible work in the CRAC. It is important to note only the shaft work for the fans was considered in this second law analysis. The DA085 CRAC units also have a scroll compressor and a refrigerant pump with a loop economizer. The data for these components are not included in the CFD library and are considered confidential by the manufacturer. Thus, we were not able to

include the exergy destruction for these components in our work. Remember that the method described in the section "Entropy production in turbulent flows for CFD" applies only to entropy generation by the flow in the room; no contribution from equipment is considered.

RESULTS

SHI and RHI

Many CFD simulations were performed and SHI and RHI calculated (see Table 4). Both metrics show mixing between the cold and hot air streams. The level of flow that is supplied to the room affects the metric values. Simulations according to the conditions given in Table 2 were made assuming maximum air flow from the CRACS and CRAC proportional flow control. (see below)

Table 4. SHI and RHI results.

		Maximum Flow		Flow Control	
	Scenarios	SHI	RHI	SHI	RHI
Room 1	1	0.40	0.60	0.57	0.43
	2	0.48	0.52	0.62	0.38
	3	0.53	0.47	0.67	0.33
Room 2	1	0.33	0.67	0.65	0.35
	2	0.47	0.53	0.67	0.33
	3	0.58	0.42	0.72	0.28
Room 3	1	0.35	0.65	0.54	0.46
	2	0.56	0.44	0.70	0.30
	3	0.59	0.31	0.70	0.30
	4	0.48	0.52	0.65	0.35

Clearly the values presented in Table 4 are far from those recommended for data centers. Short circuiting and mixing problems exist. SHI and RHI values changes with flow control demonstrate that the level of flow affect the cooling performances. Reducing the total flow rate in the room by the control system used in CRAC units generate values of SHI and RHI commonly out of the recommended ranges for data center. Mixing generates entropy and causes exergy destruction in the room as noted above (Sharma et al. [7]). Visualization of results from the CFD simulations helps to find zones of mixing generated by recirculation.

Battery reliability is affected by air temperature that surrounds the equipment. From the CFD simulations, the air temperature is obtained in the battery area for each of the rooms. In North America, 77ºF (25ºC) is the room temperature proposed for battery plants in accordance with ASHRAE [4]. Based on data from 6 Sigma [19], in order to maintain a uniform room temperature, the set point for the return air sensor at the CRAC is set to 25ºC. The air flow and temperature control is assigned to the return sensor, this is known as coupled sensor control. Using the return sensor allows measure air temperature in the room and see how far is from the temperature recommended for the batteries. Then, air flow and cooling provision are estimated with the temperature measured at that sensor.

Temperature Contour. Battery zone

Battery reliability is associated with the ambient temperature mentioned in the Introduction and the last section [3-5]. The air temperature surrounding the batteries in the simulations fluctuates between 24°C and 27°C. Low and high temperatures reduce the battery performance in the discharging process; as well as reducing battery life

As an example of this, temperature contours are plotted in Fig. 4 to highlight the air temperature that surrounds the batteries.

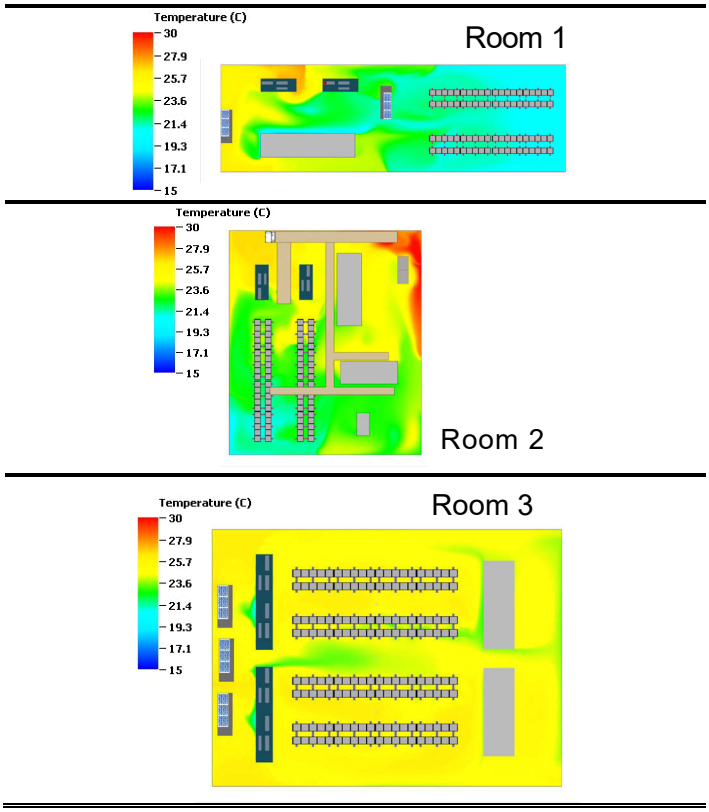

Figure 4. Temperature contour 1m from the floor.

Exergy Destruction Due to the Flow circulating in the Rooms

Kock and Herwig [16-18] developed the method described in the methodology section, thus modeling the entropy generation in turbulent flow. Silva-Llanca et al. [21] calculated the exergy destruction in a data center through two methods, direct and indirect.

In turbulent flows, eddies create fluctuations in the properties velocity, pressure, temperature, etc. These properties are decomposed by the Reynolds decomposition, where the local property is the sum of the mean and fluctuating parts. The three rooms investigated show similar tendencies in respect to exergy destruction by mean and fluctuating properties. In Room 2, the exergy destruction marks a difference in respect to the rest of the rooms in terms of the exergy destroyed by the (thermal) heat transfer through mixing. In Room 2 as well, the highest value of SHI and the

lowest values of RHI were registered. This case was extremely remote from the ideal scenario of no mixing. Exergy destruction in the rooms was obtained for air flow in the room volume. Equipment such as UPS and CRAC are modeled with compact models, for which the internal entropy generation for the equipment was not considered. Hence, the exergy obtained in this section is due to the flow distribution in the rooms. Equations (8) and (9) are used to produce the exergy destruction contour plots in the rooms.

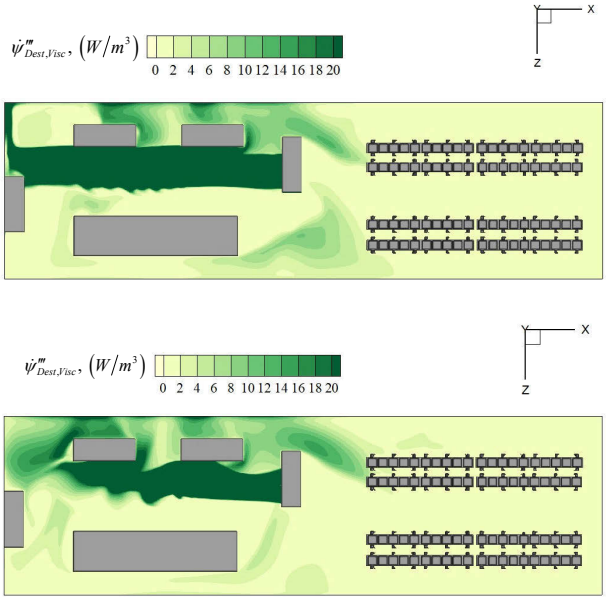

Figure 5. Exergy destruction by viscous shear effects Room 1 scenario 2, a) Maximum flow and b) Flow control.

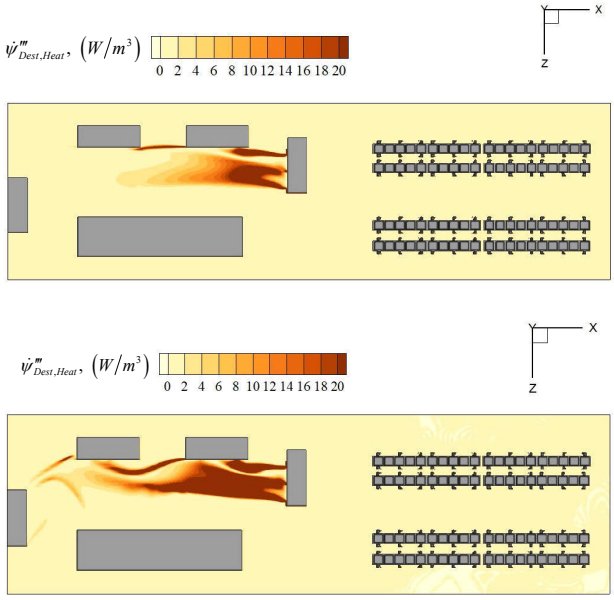

Figure 6. Exergy destruction by heat transfer Room 1 scenario 2, a) Maximum flow and b) Flow control.

Figures 5 and 6 shows how powerful the exergy destruction visualization is. Room configuration affects the zones where exergy is destroyed. Another important fact is the use of flow controller reduces the areas affected by exergy destruction (wasteful energy practices) by as much as cooled areas where it is not needed producing exergy destruction essentially by viscous dissipation.

We investigated exergy destruction with different minimum air flows while using the proportional controller. Based on information from VERIZON, the CRAC units have a recommended operating flow rate of 55% of the maximum. The percentage of maximum flow rate for a typical CRAC unit as a function of controller output that was used for this study is shown in Fig. 7.

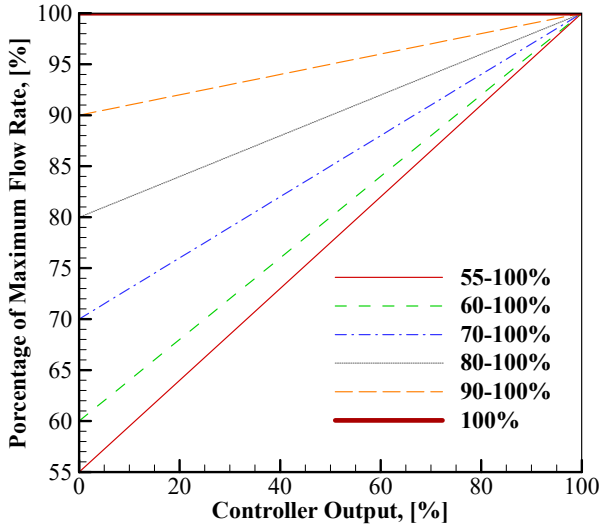

Figure 7. Proportional control.

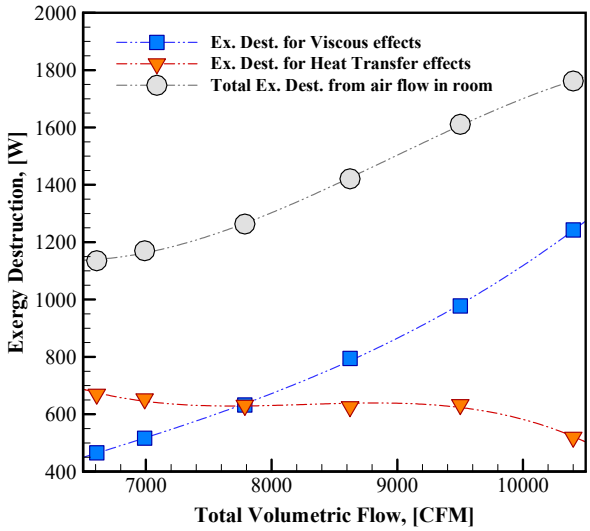

Figure 8. Exergy destroyed by total flow rate blow in Room 1 scenario 3.

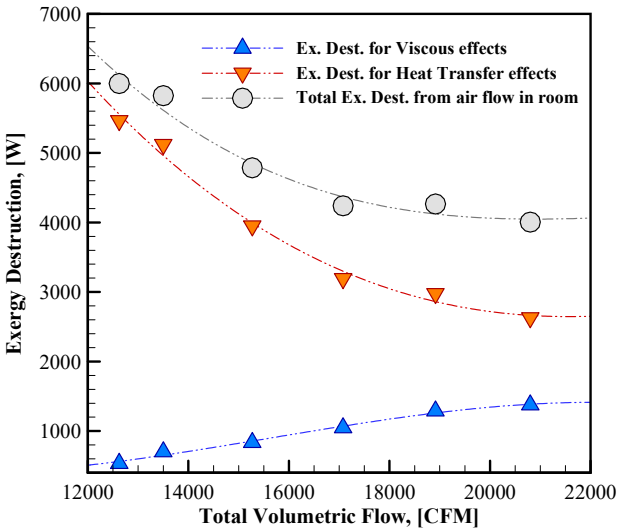

Figure 9. Exergy destroyed by total flow rate blow in Room 2 scenario 1.

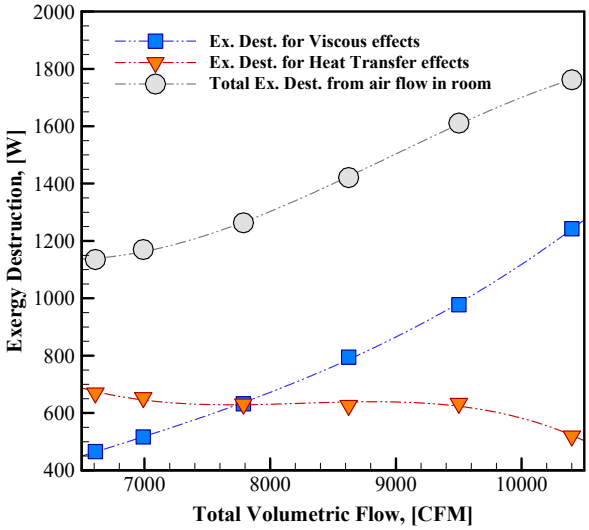

Figure 10. Exergy destroyed by total flow rate blow in Room 3 scenario 1.

By inspection of Fig. 8 and 10 above, Room 1 and Room 3 behave similarly at all flow rates because both rooms are composed of the same equipment and have similar configurations. Room 2 possesses two power distribution units. The presence of these PDUs and Room 2 configuration affects the exergy destruction by heat transfer observed in the Fig. 9. The heat dissipation by the power distribution units affect the level of exergy destruction by heat transfer given opposite behavior compared with rooms 1 and 3. The values obtained from Eqn. (10) shows that for the minimum exergy destruction is at the minimum total flow rate. However, in Room 2 the minimum exergy destroyed obtained is when the CRAC supply maximum flow rate.

Total Exergy Destruction

In the previous section, the total exergy destruction for the air flow was calculated. Using data for the CRAC units (Eqn. (11)), the exergy destruction by the CRAC units is included to obtain the total exergy destruction (see Figs. 11, 12 and 13).

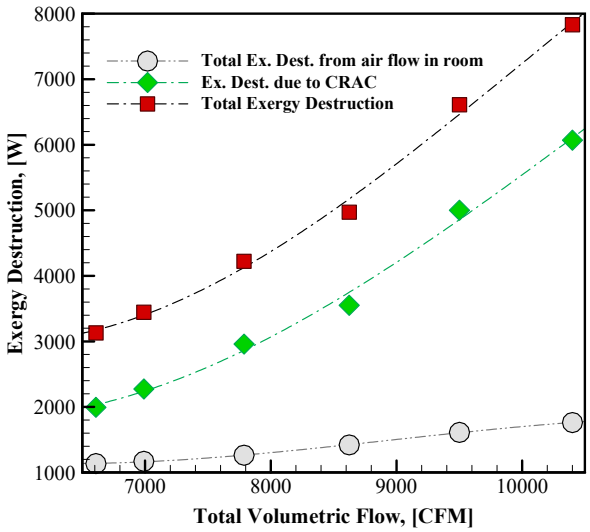

Figure 11. Total exergy destruction including the CRAC units and room air flow for Room 1 Scenario 3.

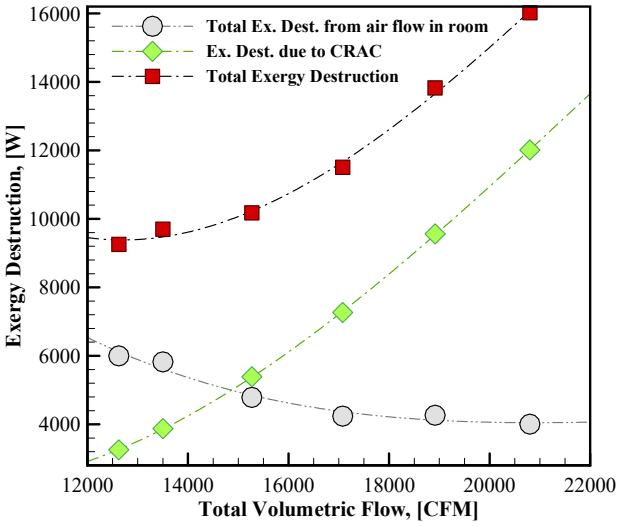

Figure 12. Total exergy destruction including the CRAC units and room air flow for Room 2 Scenario 1.

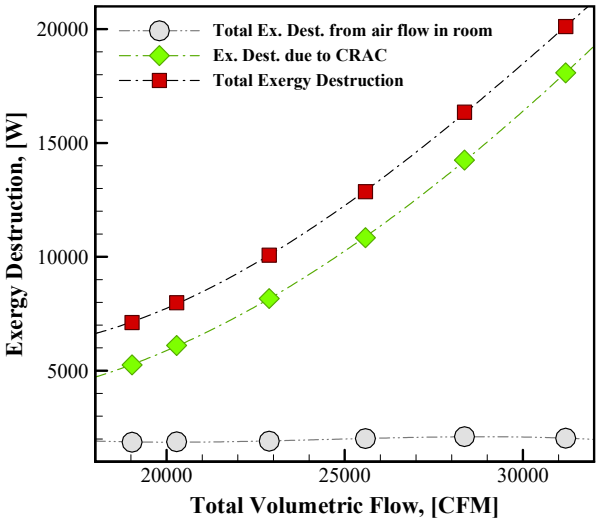

Figure 13. Total exergy destruction including the CRAC units and room air flow for Room 3 Scenario 1.

In Figs. 11, 12 and 13, we see that the exergy destruction in the CRAC units increases with total volumetric air flow rate. On the other hand, the exergy destruction trend is the opposite for viscous shear and heat transfer mixing effects for the air flow in the room. The sum of the two exergy destruction curves in Fig. 11, 12 and 13 shows that the exergy destruction increases with increased total volumetric flow rate. Therefore, maximum thermodynamic performance is obtained when the CRAC units operate at the minimum allowable air flow rate.

Summary & Conclusions

1. SHI and RHI metrics were used to characterize thermal performance in this problem. The metrics shows mixing between cold and hot air streams. Therefore, high SHI and RHI values were out of the recommended range for a good-performing room.
2. We began this study using the bulk metrics SHI and RHI. However, these do not allow us to identify local regions where the entropy generation is large and demand our attention to improve the overall thermal performance. Thus, the exergy destruction concept was introduced as a metrics of evaluation.
3. The Kock and Herwig method was used to calculate the entropy production produced by the air that circulates in the room. Internal exergy destruction by the equipment is not considered in the Kock and Herwig method.
4. Exergy destruction due to viscous shear increases when the flow rate in the room increases. This behavior was observed in all the rooms. On the other hand, exergy destruction by heat transfer slightly decreased for Room 1 and 3. In the case of Room 2, which includes two power distribution units, when the total air flow increases, the exergy destruction by heat transfer decreases.
5. Including the exergy destroyed by the CRAC, demonstrated that the minimum exergy destruction will always be at minimum air flow rate. Accordingly, the CRAC unit is a considerable source of irreversibilities in the rooms.
6. Room configuration may reduce the exergy destruction. This means that locating equipment such as UPS and CRAC units in appropriate places may reduce mixing that increase the entropy production. Within the scope of this project, little can be done to reduce the exergy destruction in the CRAC units since there are characteristics of the units themselves.
7. The method proposed by Kock and Herwig allows us to produce contour plots of exergy destruction. Hence, areas of large lost available work can be detected and changes can be made to improve the rooms.

Acknowledgments

This material is based upon the work supported by the national Science Foundation Center for Energy Smart Electronic Systems (ES2) under Grant No. IIP-1738782. Any opinions, findings, and conclusions or recommendations expressed in this material are those of the author(s) and do not necessarily reflect the views of the National Science Foundation.

References

[1] A. Capozzoli, G. Serale, L. Liuzzo, and M. Chinnici, "Thermal metrics for data centers: A critical review," Energy Procedia, vol. 62, pp. 391-400, 2014.

[2] N. F. P. Association, NFPA 70: National Electrical Code: NationalFireProtectionAssoc, 2011.

[3] "IEEE Recommended Practice for Installation Design and Installation of Vented Lead-Acid Batteries for Stationary Applications," IEEE Std 484-2002 (Revision of IEEE Std 484-1996), pp. 0_1-16, 2003.

[4] A. T. Committee, "ASHRAE TC 9.9 Thermal guidelines for data processing enviroments," ed: USA: American Society of Heating, Refrigerating and Air Conditioning Engineers Inc, 2011.

[5] "IEEE/ASHRAE Draft Guide for the Ventilation and Thermal Management of Batteries for Stationary Applications," P1635/D10/ASHARE 21/D10, December 2016, pp. 1-121, 2017.

[6] N. Rasmussen, "Calculating total cooling requirements for data centers," White paper, vol. 25, pp. 1-8, 2007.

[7] R. K. Sharma, C. E. Bash, and C. D. Patel, "Dimensionless parameters for evaluation of thermal design and performance of large-scale data centers," in 8th ASME/AIAA Joint Thermophysics and Heat Transfer Conference, 2002.

[8] A. J. Shah, V. P. Carey, C. E. Bash, and C. D. Patel, "An exergy-based control strategy for computer room air-conditioning units in data centers," in Proc. 2004

ASME International Mechanical Engineering Congress and Exposition, 2004.

[9] A. J. Shah, V. P. Carey, C. E. Bash, and C. D. Patel, "Exergy-based optimization strategies for multi-component data center thermal management: Part I—analysis," in ASME 2005 Pacific Rim Technical Conference and Exhibition on Integration and Packaging of MEMS, NEMS, and Electronic Systems collocated with the ASME 2005 Heat Transfer Summer Conference, 2005, pp. 205-213.

[10] A. J. Shah, V. P. Carey, C. E. Bash, and C. D. Patel, "An exergy-based figure-of-merit for electronic packages," Journal of Electronic Packaging, vol. 128, pp. 360-369, 2006.

[11] A. J. Shah, V. P. Carey, C. E. Bash, and C. D. Patel, "Exergy analysis of data center thermal management systems," Journal of Heat Transfer, vol. 130, p. 021401, 2008.

[12] A. J. Shah and N. Krishnan, "Optimization of global data center thermal management workload for minimal environmental and economic burden," IEEE Transactions on Components and Packaging Technologies, vol. 31, pp. 39-45, 2008.

[13] A. J. Shah and M. Meckler, "An exergy-based framework for assessing sustainability of it systems," in ASME 2009 3rd International Conference on Energy Sustainability collocated with the Heat Transfer and InterPACK09 Conferences, 2009, pp. 823-832.

[14] A. J. Shah and C. D. Patel, "Designing environmentally sustainable electronic cooling systems using exergo-thermo-volumes," International Journal of Energy Research, vol. 33, pp. 1266-1277, 2009.

[15] A. J. Shah and C. D. Patel, "Exergo-thermo-volumes: an approach for environmentally sustainable thermal management of energy conversion devices," Journal of Energy Resources Technology, vol. 132, p. 021002, 2010.

[16] F. Kock and H. Herwig, "Local entropy production in turbulent shear flows: a high-Reynolds number model with wall functions," International Journal of Heat and Mass Transfer, vol. 47, pp. 2205-2215, 2004.

[17] F. Kock and H. Herwig, "Entropy production calculation for turbulent shear flows and their implementation in CFD codes," International Journal of Heat and Fluid Flow, vol. 26, pp. 672-680, 2005.

[18] H. Herwig and F. Kock, "Direct and indirect methods of calculating entropy generation rates in turbulent convective heat transfer problems," Heat and mass transfer, vol. 43, pp. 207-215, 2007.

[19] F. Facilities, "6Sigma DCX 11, User Manual ", ed. San Jose, CA, USA, 2017.

[20] A. Bejan, Entropy generation minimization: the method of thermodynamic optimization of finite-size systems and finite-time processes: CRC press, 1995.

[21] L. Silva-Llanca, A. Ortega, K. Fouladi, M. del Valle, and V. Sundaralingam, "Investigation of exergy destruction in CFD modeling for a legacy air-cooled data center," in Thermal and Thermomechanical Phenomena in Electronic Systems (ITherm), 2014 IEEE Intersociety Conference on, 2014, pp. 1366-1374.

[22] Silva-Llanca, L., Ortega, A., Fouladi, K., del Valle, M., & Sundaralingam, V. (2018). "Determining wasted energy in the airside of a perimeter-cooled data center via direct computation of the Exergy Destruction". Applied Energy, 213, 235-246.